

Coronal Magnetic Field Extrapolation Using a Specific Family of Analytical 3D MHS Equilibria

L. Nado¹, T. Neukirch¹, T. Wiegmann²

¹ *School of Mathematics and Statistics, University of St Andrews, St Andrews, UK*

² *Max-Planck-Institute for Solar System Research, Göttingen, Germany*

Coronal magnetic field models have to rely on extrapolation methods using photospheric magnetograms as boundary conditions. In recent years, due to the increased resolution of observations and the need to resolve non-force-free lower regions of the solar atmosphere, there have been increased efforts to use MHS field models instead of force-free methods. Although numerical methods can deal with non-linear problems and provide accurate models, analytical three-dimensional MHS equilibria can be used as a numerically relatively “cheap” complementary method. We discuss a family of analytical MHS equilibria that allows for a transition from a non-force-free to a force-free region based on the MHS equations

$$\mathbf{j} \times \mathbf{B} - \nabla p - \rho \nabla \Psi = 0, \quad \nabla \times \mathbf{B} = \mu_0 \mathbf{j}, \quad \nabla \cdot \mathbf{B} = 0$$

and the current density being represented by $\mu_0 \mathbf{j} = \alpha \mathbf{B} + \nabla \times (F \hat{\mathbf{z}})$ with $F = f(z) B_z$ (see e.g. [1, 2]) using standard notation. Such that the dependence of the non-force-free part of \mathbf{j} with height z is controlled by $f(z)$. Neukirch and Raststätter (1999) [3] have shown that for a magnetic field of the form

$$\mathbf{B} = \nabla \times [\nabla \times (\Phi \hat{\mathbf{z}})] + \alpha \nabla \times (\Phi \hat{\mathbf{z}})$$

a solution is given by

$$\Phi = \iint_{-\infty}^{\infty} \bar{\Phi}(z; k_x, k_y) \exp[i(k_x x + k_y y)] dk_x dk_y \quad (1)$$

where $\bar{\Phi}$ obeys the differential equation

$$\frac{d^2 \bar{\Phi}}{dz^2} + [\alpha^2 - k^2 + k^2 f(z)] \bar{\Phi} = 0 \quad (2)$$

with $k^2 = k_x^2 + k_y^2$ (see [4]). If periodic boundary conditions in x and y are imposed k_x and k_y take on discrete values and the integrals in Eq. (1) are represented by infinite sums. Neukirch and Wiegmann (2019) [4] have used $f(z) = a[1 - b \tanh((z - z_0)/\Delta z)]$ where a and b control the magnitude of f in the domains $\frac{z - z_0}{\Delta z} \ll 0$ and $\frac{z - z_0}{\Delta z} \gg 0$, z_0 is the centre of the transitional region and Δz controls the width over which the transition happens. Hence, (2) becomes

$$\frac{d^2 \bar{\Phi}}{dz^2} + \left[\alpha^2 - k^2 (1 - a) - k^2 ab \tanh\left(\frac{z - z_0}{\Delta z}\right) \right] \bar{\Phi} = 0 \quad (3)$$

Neukirch and Wiegelmann (2019) [4] have used the hypergeometric function ${}_2F_1(a, b, c; z)$ (see [5]) to find a solution of (3) given by

$$\begin{aligned}\bar{\Phi} = & \tilde{A}\eta^{\tilde{\delta}}(1-\eta)^{\tilde{\gamma}} {}_2F_1\left(\tilde{\gamma} + \tilde{\delta} + 1, \tilde{\gamma} + \tilde{\delta}, 2\tilde{\delta} + 1, \eta\right) \\ & + \tilde{B}\eta^{-\tilde{\delta}}(1-\eta)^{\tilde{\gamma}} {}_2F_1\left(\tilde{\gamma} - \tilde{\delta} + 1, \tilde{\gamma} - \tilde{\delta}, 1 - 2\tilde{\delta}, \eta\right)\end{aligned}$$

with $\tilde{\gamma} = \sqrt{C_2}$ and $\tilde{\delta} = \sqrt{C_1}$ and $C_{1,2} = \frac{1}{4} [\bar{k}^2 (1 - a \pm ab) + \bar{\alpha}^2]$ with $\bar{k} = k\Delta z$ and $\bar{\alpha} = \alpha\Delta z$. The constants \tilde{A} and \tilde{B} are determined by the boundary conditions. While routines for the calculation of the hypergeometric function ${}_2F_1$ are available, these can affect both the speed and the accuracy of the calculations. Therefore, we look into the asymptotic behaviour of this solution in order to approximate it through exponential functions aiming to improve the numerical efficiency.

We define $\omega = \frac{z-z_0}{\Delta z}$. For small Δz the value of the hyperbolic tangent depends on the sign of its argument. Hence, we distinguish between $z - z_0 > 0$ and $z - z_0 < 0$. Eq. (3) then reduces to

$$\frac{d^2\bar{\Phi}}{dz^2} + [\alpha^2 - k^2(1 - a \pm ab)]\bar{\Phi} = 0 \quad (4)$$

where we have $+ab$ for positive $z - z_0$ and $-ab$ for negative $z - z_0$. We define

$$-4C_{\pm} = \alpha^2 - k^2(1 - a \pm ab)$$

We define $\sqrt{C_+} = \delta$ and $\sqrt{C_-} = \gamma$ and assume $C_+, C_- > 0$. A solution of Eq. (4) is then given by

$$\bar{\Phi} = \begin{cases} A \exp(2\delta z) + B \exp(-2\delta z), & z - z_0 > 0 \\ A' \sinh(2\gamma z) + B' \cosh(2\gamma z), & z - z_0 < 0 \end{cases}$$

We consider a coordinate transformation and apply the following boundary conditions: (1) As z goes to infinity we want $\bar{\Phi}$ to vanish. (2) We want $\bar{\Phi}$ to be a continuously differentiable function. (3) We want $\bar{\Phi} \equiv 1$ at $z = 0 = z_{min} < z_0$. Then we have

$$\bar{\Phi} = \frac{1}{D} \begin{cases} \exp\left(-\frac{2\delta}{\Delta z}(z - z_0)\right), & z - z_0 > 0 \\ \frac{\delta}{\gamma} \sinh\left(\frac{2\gamma}{\Delta z}(z_0 - z)\right) + \cosh\left(\frac{2\gamma}{\Delta z}(z_0 - z)\right), & z - z_0 < 0 \end{cases}$$

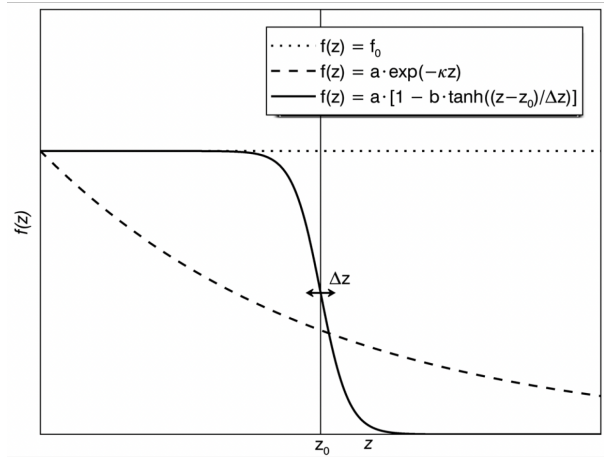


Figure 1: From [4]. Different versions of $f(z)$. The exponential profile was introduced by Low (1991, 1992) [1, 2] and is applied successfully frequently. The hyperbolic tangent profile allows for more flexibility and unlike the Low solution reaches a purely force-free state eventually.

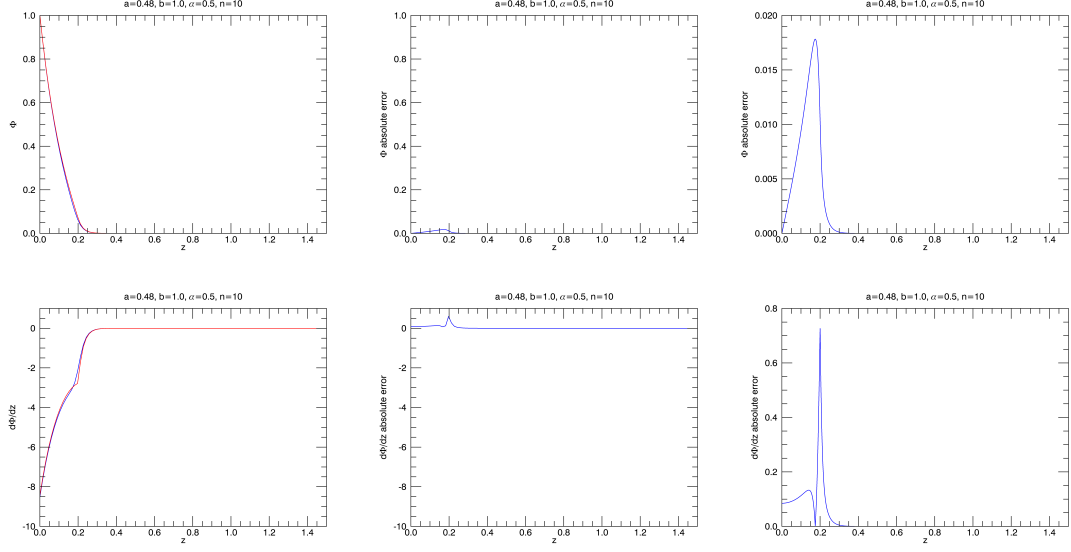


Figure 2: Φ and $d\Phi/dz$ for $n = 10$, $\alpha = 0.5$, $a = 0.24$, $b = 1.0$, $z_0 = 0.2$ and $\Delta z = 0.02$.

and

$$\bar{\Phi}' = -\frac{1}{D} \begin{cases} \frac{2\delta}{\Delta z} \exp\left(-\frac{2\delta}{\Delta z}(z - z_0)\right), & z - z_0 > 0 \\ \frac{\delta}{\gamma} \frac{2\gamma}{\Delta z} \cosh\left(\frac{2\gamma}{\Delta z}(z_0 - z)\right) + \frac{2\gamma}{\Delta z} \sinh\left(\frac{2\gamma}{\Delta z}(z_0 - z)\right), & z - z_0 < 0 \end{cases}$$

In Figure 2 we see the asymptotic solution in red and the analytic solution in blue plotted for the tenth Fourier mode in an MHS setting ($a = 0.24$, $\alpha = 0.5$). The largest difference occurs around z_0 and generally in the MHS part of the model rather than in the force-free part of the model. While the maximum errors of order of 1 in the derivative are large - even when put in relation to the values of the function itself - we keep in mind that we are more interested in the error that occurs in the field lines and in the plasma parameters when calculated with the red instead of the blue function. In Figure 3 we see the maximum absolute difference between the plasma parameters calculated with the exact solution and calculated with the asymptotic solution. The red graph has been calculated with $\Delta z = 0.1$, blue with $\Delta z = 0.05$ and green with $\Delta z = 0.02$. We see that the error in pressure and density are of the magnitude of 10^{-4} and 10^{-3} , respectively. For both quantities the error decreases with decreasing value of Δz . This implies that we are able to use Δz to control the error in the plasma parameters. In this setting 0.01 on the z -scale (so relevant for z_0 and Δz) corresponds to 100 kilometres in the solar atmosphere. So far, we have modelled magnetic field lines on periodic boundary conditions. The calculation using the asymptotic Φ is at least six times faster than using the original solution and component-wise comparison of the magnetic field vectors for the exact and the asymptotic model has shown that their average difference is of the order of 10^{-6} . In conclusion, we are using a magnetic field model for the solar atmosphere that includes the transition from non-force-

free to force-free (from photosphere to corona) using a special function that allows for more flexibility than commonly used methods. We substituted the exact solution with its asymptotic approximation, which improved the efficiency of the model without compromising on accuracy.

We plan to test the code with different boundary magnetic fields, e.g. unbalanced or multi-source. Ultimately, we intend to apply our model to observational data and to compare those results with results obtained using solutions for other functions $f(z)$ (e.g. [1, 2]).

LN acknowledges financial support by the University of St Andrews, and TN acknowledges support by the United Kingdom's Science and Research Council (STFC) via Consolidated Grant ST/W001195/1.

References

- [1] B. Low, The Astrophysical Journal **370**, 427-434 (1991)
- [2] B. Low, The Astrophysical Journal **399**, 300-312 (1992)
- [3] T. Neukirch and L. Rastätter, Astronomy and Astrophysics **348**, 1000-1004 (1999)
- [4] T. Neukirch and T. Wiegmann, Solar Physics **294**, 1-18 (2019)
- [5] NIST Digital Library of Mathematical Functions, 2014, <https://dlmf.nist.gov/15>

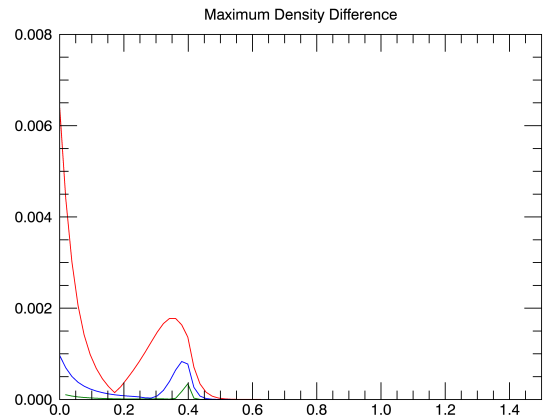
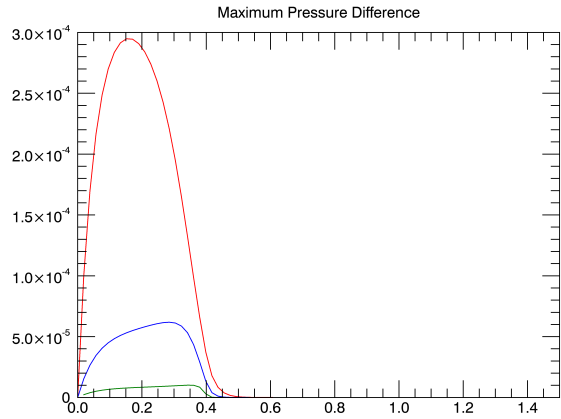


Figure 3: Maximum differences in pressure and density between the two models with $\alpha = 0.5$, $a = 0.24$, $b = 1.0$, $n_{\text{resol}} = 30$, $n_f = 20$, $z_0 = 0.4$, $\Delta z = 0.1, 0.05, 0.02$. The x axis represents the height z from photosphere to corona.